

Original Article

Alterations in gene expression precede sarcopenia and osteopenia in botulinum toxin immobilized mice

J.B. Vegger, A. Brüel, A.F. Dahlgaard, J.S. Thomsen

Department of Biomedicine, Aarhus University, Wilhelm Meyers Allé 3, DK-8000 Aarhus C, Denmark

Abstract

Objectives: To investigate alteration of bone and muscle gene expression at different time points during 3 weeks of botulinum toxin (BTX) induced immobilization and how this correlate with conventional analysis of bone and muscle. **Methods:** Thirty-five 16-week-old female C57BL/6-mice were investigated; 15 were injected with BTX, 15 served as age-matched controls, and 5 as baseline. 5 BTX-injected and 5 control mice were euthanized after 1, 2, and 3 weeks. Analysis included RT-qPCR, dynamic bone histomorphometry, DEXA, μ CT, mechanical testing, and muscle cell cross-sectional-area (CSA). **Results:** Genes related to osteoblasts were expressed at a lower level after 1 week, but not after 2 and 3 weeks of disuse. Moreover, genes related to osteoclasts were expressed at a higher level after 1 and 2 weeks of disuse, whereafter they approached the level of the controls. Genes related to muscle atrophy were upregulated 1 and 2 weeks after the BTX-injection, but not after 3 weeks. In contrast, deterioration of bone microstructure and strength, and reduction in muscle cell CSA were most evident after 3 weeks of disuse. **Conclusions:** Gene expression should be investigated during the first two weeks of immobilization, whereas changes in bone microstructure and muscle cell CSA are most prominent after 3 weeks of immobilization.

Keywords: Immobilization, Mice, Gene Expression, MicroCT, Mechanical Testing

Introduction

Several animal models have been used to study the impact of immobilization on bone homeostasis e.g. plaster casting, elastic bandaging, surgical denervation, hind limb suspension or, as in the present study, injection of botulinum toxin (BTX)¹⁻⁴. The BTX model of immobilization has repeatedly been shown, by us and others, to induce a rapid and severe bone loss in rodents⁴⁻¹¹. In mice, the maximum bone loss is seen 3-4 weeks after injection with BTX^{12,13}. However, it is unknown how expression of relevant genes correlates with conventional methods of bone analysis like dynamic histomorphometry, DEXA, μ CT, and mechanical

testing. The ideal time point to analyze gene expression may not be when major changes are seen at tissue level, as disuse induced alterations in gene expression most likely to take place prior to deterioration of bone microarchitecture and bone strength.

In bone, *Bglap* (osteocalcin) and *Col1a1* (collagen, type 1, alpha 1) are expressed by osteoblasts and are closely related to bone formation¹⁴. The transcription of *Runx2* (runt-related transcription factor 2) is important for osteoblastic differentiation¹⁵. *Sost* (sclerostin) is expressed by osteocytes, and its product sclerostin is an inhibitor of bone formation as an antagonist of the Wnt signaling pathway¹⁶. Moreover, the expression of *Sost* has been linked to mechanical unloading^{17,18}. *Ctsk* (cathepsin K) and *Acp5* (tartrate-resistant acid phosphatase type 5), and their products, are closely related to the function of osteoclasts and bone resorption^{19,20}. The ratio between *Rankl* (receptor activator of nuclear κ -B ligand) and *Opg* (osteoprotegerin), and their products, are important in orchestrating bone resorption²¹. Investigating the expression of the above mentioned genes will provide an overview of the cellular mechanisms and activities occurring during immobilization induced bone loss.

The authors have no conflict of interest.

Corresponding author: Jens Bay Vegger, Department of Biomedicine, Aarhus University, Wilhelm Meyers Allé 3, DK-8000 Aarhus C, Denmark
E-mail: jbve@biomed.au.dk

Edited by: M. Hamrick
Accepted 7 July 2016



Likewise, it is unknown how gene expression in muscles injected with BTX correlates with muscle atrophy and bone loss. The expression of *Murf1* (tripartite motif-containing 63) and *Atrogin1* (F-box protein 32) increase during muscle atrophy and are therefore ideal for this investigation. The function of the translated products of *Murf1* and *Atrogin1* are to bind specific substrates within muscle cells and mark these substrates for proteasome degradation²².

The aim of the present study was to investigate alteration of bone and muscle gene expression at different time points during the first 3 weeks of botulinum toxin (BTX) induced immobilization and how these alterations correlate with the subsequent changes in conventional bone parameters as obtained by dynamic bone histomorphometry, DEXA, μ CT, mechanical testing as well as muscle parameters such as muscle weight and muscle cell cross-sectional-area compared to control animals.

Materials and methods

Animals

Thirty-five 16-week-old female C57BL/6 mice (Taconic) with a mean body weight of 23.4 ± 1.1 g were housed at 20°C with a 12/12 h light/dark cycle. The animals had free access to standard mice chow (1324, Altromin) and tap water.

At the age of 15 weeks, one week prior to study start, the animals were randomized according to their body weight (BW) into seven groups with 5 mice in each group: one Baseline (Base), three Control (Ctrl), and three BTX groups. At study start, the mice in the BTX groups were injected i.m. with 2 IU/100 g BW BTX (Botox, Allergan), distributed equally into the quadriceps muscle and calf muscles of the right hind limb⁶. The Ctrl groups were injected with saline using the same regimen as for the BTX injections. The mice were injected i.p. with alizarin (20 mg/kg) 6 and 2 days before euthanasia.

The mice were euthanized by anesthesia (IsoFlo Vet, Orion Pharma Animal Health) and removal of the heart. No mice died prematurely. The Base group was euthanized at study start and served as baseline. Then one Ctrl and BTX group was euthanized after 7, 14, and 21 days of immobilization.

Immediately after euthanasia, the tibiae were quickly isolated, cleaned from soft tissue, divided into a proximal and distal part, and snap frozen at -80°C. In addition, the rectus femoris muscles were isolated, and the wet weight determined. Then, the rectus femoris muscle was cut in two, and either snap frozen at -80°C or immersion-fixed in 0.1 M sodium phosphate buffered formaldehyde (4% formaldehyde, pH 7.0). The femora were isolated, carefully cleaned from soft connective tissue, and stored in Ringer's solution at -20°C. The experiment complied with the EU Directive 2010/63/EU for animal experiment, and all procedures were approved by the Danish Animal Experiments Inspectorate.

Dual energy x-ray absorptiometry (DEXA)

The length of the femora was measured with a digital sliding caliper, and the femora were then placed in a DEXA scanner (Sabre XL, Norland Stratec), and scanned with an isotropic pixel size of 0.1 mm. Bone mineral content (BMC) and areal bone mineral density (aBMD) were determined for the whole femur. Quality assurance was performed by scans of the two solid-state phantoms provided with the scanner.

Micro computed tomography (μ CT)

The mid-femoral diaphysis and distal femur were scanned in a desktop μ CT scanner (Scanco μ CT 35, Scanco Medical AG). The mid-femoral diaphysis was scanned with an isotropic voxel size of 7 μ m, a X-ray tube voltage of 55 kV and current of 145 μ A, and an integration time of 300 ms, while the distal femur was scanned with an isotropic voxel size of 3.5 μ m, a X-ray tube voltage of 55 kV and current of 145 μ A, and an integration time of 800 ms.

The femoral mid-diaphysis was analyzed by semi automatically drawing an 819- μ m-high volume of interest (VOI) including cortical bone only with the software provided with the μ CT scanner (version 6.5, Scanco Medical AG). The 3D data sets were low-pass filtered using a Gaussian filter ($\sigma=0.8$, support=1) and segmented with a fixed threshold filter (556.4 mg HA/cm³). The analysis included: bone area, tissue area, marrow area, polar moment of inertia (pMOI), and bone material density (ρ). The areas were found as volumes divided by the height of the VOI.

The distal femoral metaphyses were analyzed by semi manually drawing a 1-mm-high VOI including trabecular bone, but excluding cortical bone, placed 0.2 mm proximal to the growth plate. The 3D data sets were low-pass filtered using a Gaussian filter ($\sigma=1$, support=2) and segmented with a fixed threshold filter (447.6 mg HA/cm³). The distal femoral epiphysis was analyzed by semi manually drawing a VOI placed distal to the growth plate, including trabecular bone only, until the protrusion of the condyles. The 3D data sets were low-pass filtered using a Gaussian filter ($\sigma=1$, support=2) and segmented with a fixed threshold filter (537.9 mg HA/cm³). The analysis included: bone volume fraction (BV/TV), trabecular thickness (Tb.Th), trabecular number (Tb.N), trabecular separation (Tb.Sp), connectivity density (CD), structure model index (SMI) as previously described in detail²⁴, as well as bone material density (ρ). For each skeletal site the minimum point between the marrow and the bone peak in the attenuation histogram was automatically determined using IPL (version 5.11, Scanco Medical AG) and the median of these thresholds was used as threshold for all bones at the respective skeletal site.

The bone analyzes were conducted in compliance with the current guidelines²³. Quality assurance was performed by weekly (density) and monthly (geometry) scans of the solid-state calibration phantom provided with the scanner.

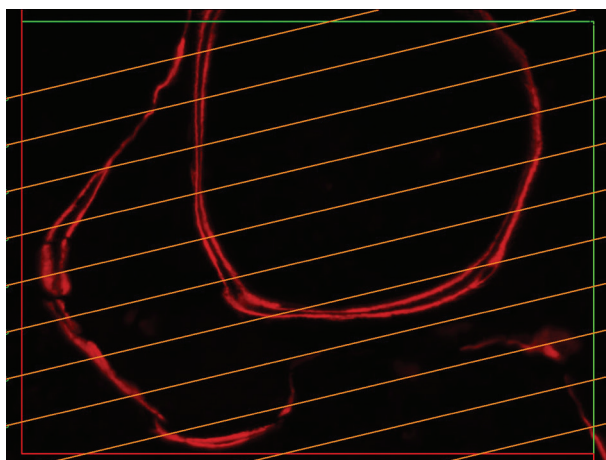


Figure 1. Screenshot of the stereology system newCAST (Version 4.6.3.857, Visiopharm) showing the line grid used during live acquisition of dynamic bone histomorphometry data at a magnification of $\times 1170$.

Mechanical testing

The fracture strength of the femoral mid-diaphysis was determined with a three-point bending test. The femora were placed on a custom made testing jig, supporting the proximal and distal part of the shaft. The distance between the two supporting rods was 7.1 mm. Load was applied at the midpoint of the femur at a constant deflection rate of 2 mm/min until fracture using a materials testing machine (5566, Instron).

Subsequently, the proximal half of the femur was placed in another custom made fixation jig supporting the shaft under the neck. Load was applied to the top of the femoral head with a constant deflection rate of 2 mm/min until fracture of the femoral neck.

Dynamic bone histomorphometry

After mechanical testing, the distal femoral metaphysis were immersion-fixed in 0.1 M sodium phosphate buffered formaldehyde (4% formaldehyde, pH 7.0) for 48 h, dehydrated in ethanol, embedded undecalcified in methylmetacrylate, and 7- μm -thick sections were cut using a hard tissue microtome (Leica RM 2065). The sections were mounted unstained on microscope slides and placed in a microscope (Nikon Eclipse 80i) equipped for fluorescence microscopy. The stereology system newCAST (Version 4.6.3.857, Visiopharm) was then used to count intersections with fluorochrome labels.

Briefly, a region of interest (ROI), excluding cortical bone, was drawn semi-automatically at the distal femoral epiphysis. Furthermore, a 1000- μm -high ROI, excluding cortical bone and primary spongiosa, was placed 200 μm proximal to the distal femoral growth plate covering the distal femoral

Table 1.

	Final bodyweight (g)	Rectus femoris muscleweight (mg)	Femur length (mm)
Day 0			
Base	24.1 \pm 1.9	73.7 \pm 4.4	15.6 \pm 0.2
Day 7			
Ctrl	23.8 \pm 1.3	69.0 \pm 8.9	15.9 \pm 0.2
BTX	21.7 \pm 0.6 ^{a,b}	52.7 \pm 2.6 ^{a,b}	15.6 \pm 0.1 ^b
Day 14			
Ctrl	23.9 \pm 1.0	69.4 \pm 4.9	15.7 \pm 0.2
BTX	21.7 \pm 0.7 ^{a,b}	35.9 \pm 2.4 ^{a,b}	15.7 \pm 0.2
Day 21			
Ctrl	24.1 \pm 1.0	69.3 \pm 6.7	15.8 \pm 0.2
BTX	21.9 \pm 0.7 ^{a,b}	33.1 \pm 2.5 ^{a,b}	15.5 \pm 0.2

^a denotes a significant difference from Base and ^b denotes a significant difference from the respective Ctrl group. n=5. Mean \pm SD.

Table 2.

	BMC (mg)	aBMD (mg/cm ²)
Day 0		
Base	0.016 \pm 0.001	0.047 \pm 0.002
Day 7		
Ctrl	0.017 \pm 0.001	0.050 \pm 0.003
BTX	0.014 \pm 0.001 ^{a,b}	0.044 \pm 0.004 ^b
Day 14		
Ctrl	0.017 \pm 0.001	0.049 \pm 0.002
BTX	0.013 \pm 0.001 ^{a,b}	0.040 \pm 0.002 ^{a,b}
Day 21		
Ctrl	0.017 \pm 0.001	0.049 \pm 0.001
BTX	0.012 \pm 0.001 ^{a,b}	0.040 \pm 0.002 ^{a,b}

DXA data of the whole femur. ^a denotes a significant difference from Base and ^b denotes a significant difference from the respective Ctrl group. n=5. Mean \pm SD.

metaphysis. At a magnification of $\times 1170$, a line grid was superimposed onto fields of view that covered 50% of the ROI. The line grid was used to count intersections and distances between the fluorochrome labels (Figure 1). The counting was performed in a randomized and blinded manner. Mineralizing surfaces (MS/BS), mineral apposition rate (MAR), and bone formation rate (BFR/BS) were determined.

Table 3.

	Bone area (mm ²)	Tissue area (mm ²)	Marrow area (mm ²)	pMOI (mm ⁴)	ρ (mg/cm ³)
Day 0					
Base	0.77±0.05	1.75±0.09	0.97±0.05	0.36±0.04	1133±11
Day 7					
Ctrl	0.77±0.04	1.76±0.10	0.99±0.06	0.36±0.04	1145±7
BTX	0.74±0.03	1.76±0.04	1.02±0.03	0.35±0.02	1143±11
Day 14					
Ctrl	0.79±0.04	1.76±0.05	0.97±0.05	0.37±0.02	1154±7 ^a
BTX	0.73±0.01 ^b	1.77±0.03	1.04±0.03 ^{a,b}	0.35±0.01	1145±17
Day 21					
Ctrl	0.82±0.05	1.80±0.05	0.98±0.02	0.39±0.03	1158±10 ^a
BTX	0.70±0.03 ^{a,b}	1.78±0.06	1.07±0.03 ^{a,b}	0.34±0.03 ^b	1150±17

μCT data of cortical bone obtained from the femoral mid-diaphysis. ^a denotes a significant difference from Base and ^b denotes a significant difference from the respective Ctrl group. n=5. Mean±SD.

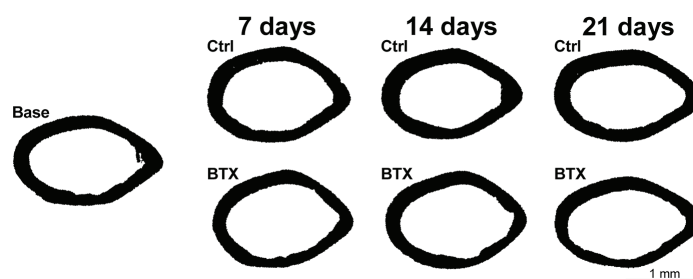


Figure 2. Representative illustrations of the femoral mid-diaphysis acquired from the μCT scans.

RT-qPCR

The distal part the tibia was ground in a 1.5 ml microcentrifuge tube with a micropestle (VWR) at -80°C. Lysis buffer from a PureLink RNA Mini kit (Ambion, LifeTechnologies) was added, and the pulverized bone was homogenized with rotor/stator homogenizer (VDI 12, VWR). RNA was isolated and purified with the PureLink RNA Mini kit. RNA quality was checked by running 1 μg total RNA on an agarose gel. 1 μg total RNA was transcribed into cDNA using qScript cDNA SuperMix (Quanta Biosciences). qPCR was carried out on a LightCycler 480 (Ver. 1.5, Roche) using TaqMan Gene Expression Assays (LifeTechnologies). cDNA was diluted 1:5 with DEPC-treated water, and 2 μl diluted cDNA was used in each reaction. PerfeCTa qPCR FastMix II (Quanta Biosciences) was used with the following amplification protocol; hot start 95°C for 30 s followed by 40 cycles of amplification and quantification at 95°C for 3 s and 60°C for 30 s. The studied genes were *Bglap* (osteocalcin), *Col1a1* (collagen, type 1, alpha 1), *Runx2* (runt-re-

lated transcription factor 2), *Sost* (sclerostin), *Ctsk* (cathepsin K), *Acp5* (tartrate resistant acid phosphatase type 5), *Rankl* (receptor activator of nuclear kappa-B ligand), and *Opg* (osteoprotegerin). Each sample was investigated in triplicates, and normalized to the reference genes *B2m* (beta-2 microglobulin) and *Gapdh* (glyceraldehyde-3-phosphate dehydrogenase). Furthermore, the ratio between the expression of *Rankl* and *Opg* was calculated i.e. the *Rankl/Opg*-ratio. Relative gene expression was quantified using the ΔΔCT method²⁵.

The frozen rectus femoris muscle specimen was homogenized in lysis buffer from the PureLink RNA Mini kit with a Bullet Blender (BBY24M, Next Advance). RNA was isolated and purified with the PureLink RNA Mini kit. 0.1 μg total RNA was transcribed into cDNA using the qScript cDNA SuperMix. qPCR was carried out on the LightCycler using TaqMan Gene Expression Assays. cDNA was diluted 1:2 with DEPC-treated water, and 3 μl diluted cDNA was used in each reaction. PerfeCTa qPCR FastMix II was used with the following amplifica-

Table 4.

	BV/TV (%)	Tb.Th (μm)	Tb.N (1/mm)	Tb.Sp (μm)	CD (1/mm ³)	SMI	ρ (mg/cm ³)
Distal femoral metaphysis							
Day 0							
Base	6.4 \pm 1.2	35.5 \pm 3.5	3.6 \pm 0.3	277 \pm 22	198 \pm 31	2.2 \pm 0.1	863 \pm 23
Day 7							
Ctrl	6.6 \pm 1.1	36.7 \pm 4.6	3.5 \pm 0.1	289 \pm 7	178 \pm 24	2.2 \pm 0.1	858 \pm 20
BTX	5.1 \pm 1.0 ^a	28.0 \pm 1.9 ^{a,b}	3.3 \pm 0.2	300 \pm 19	181 \pm 41	2.1 \pm 0.1	836 \pm 21
Day 14							
Ctrl	6.0 \pm 1.3	37.7 \pm 2.4	3.4 \pm 0.1	298 \pm 4.4	161 \pm 34	2.3 \pm 0.2	871 \pm 6
BTX	4.0 \pm 0.5 ^{a,b}	25.3 \pm 1.7 ^{a,b}	3.3 \pm 0.2	303 \pm 17	159 \pm 12 ^a	2.1 \pm 0.1	826 \pm 20 ^{a,b}
Day 21							
Ctrl	5.4 \pm 1.0	36.2 \pm 4.3	3.3 \pm 0.3	307 \pm 23	142 \pm 36 ^a	2.3 \pm 0.2	869 \pm 26
BTX	3.4 \pm 0.5 ^{a,b}	25.8 \pm 2.0 ^{a,b}	3.2 \pm 0.1 ^a	313 \pm 15 ^a	135 \pm 12 ^a	2.3 \pm 0.1	824 \pm 14 ^{a,b}
Distal femoral epiphysis							
Day 0							
Base	21.8 \pm 1.7	52.2 \pm 1.9	5.2 \pm 0.5	210 \pm 14	292 \pm 45	0.3 \pm 0.1	966 \pm 20
Day 7							
Ctrl	22.0 \pm 1.1	54.9 \pm 2.2	5.0 \pm 0.3	221 \pm 11	265 \pm 90	0.3 \pm 0.1	969 \pm 11
BTX	14.8 \pm 1.9 ^{a,b}	39.7 \pm 5.6 ^{a,b}	4.5 \pm 0.2 ^{a,b}	236 \pm 15 ^a	316 \pm 46	0.6 \pm 0.1 ^{a,b}	950 \pm 21
Day 14							
Ctrl	23.1 \pm 1.0	58.8 \pm 1.8 ^a	5.1 \pm 0.3	217 \pm 12	251 \pm 33	0.2 \pm 0.3	978 \pm 8
BTX	9.6 \pm 1.6 ^{a,b}	31.7 \pm 2.0 ^{a,b}	4.1 \pm 0.3 ^{a,b}	254 \pm 17 ^{a,b}	329 \pm 51 ^b	1.1 \pm 0.2 ^{a,b}	921 \pm 18 ^{a,b}
Day 21							
Ctrl	21.3 \pm 1.0	54.9 \pm 1.7 ^a	4.7 \pm 0.5	233 \pm 19	229 \pm 61	0.3 \pm 0.1	977 \pm 10
BTX	8.1 \pm 0.9 ^{a,b}	31.8 \pm 2.2 ^{a,b}	4.1 \pm 0.2 ^{a,b}	254 \pm 12 ^a	315 \pm 60	1.3 \pm 0.1 ^{a,b}	911 \pm 9 ^{a,b}

μCT data of trabecular bone obtained from the distal femoral metaphysis and distal femoral epiphysis. ^a denotes a significant difference from Base and ^b denotes a significant difference from the respective Ctrl group. n=5. Mean \pm SD.

tion protocol: hot start 95°C for 30 s followed by 40 cycles of amplification and quantification at 95°C for 3 s and 60°C for 30 s. Each specimen was investigated in triplicates, and the studied genes were *Murf1* (tripartite motif-containing 63) and *Atrogin1* (F-box protein 32) normalized to the reference gene *Tbp* (TATA-binding protein) according to Nakao et al.²⁶. Relative gene expression was quantified using the $\Delta\Delta\text{CT}$ method²⁵.

CSA of rectus femoris muscle cells

The formaldehyde fixed rectus femoris muscle specimens were dehydrated in ethanol, embedded in paraffin, and cut into 4- μm -thick sections with a microtome (Leica RM 2165). The sections were stained with hematoxylin and eosin, placed in the Nikon microscope, and the cross sectional area (CSA) of the muscle cells was estimated with the newCAST stereology system as earlier described⁸.

Statistics

Differences between the Base, BTX, and the respective Ctrl groups were analyzed by an independent samples Student's *t*-test, whenever normal distribution was met or else by a non-parametric Mann-Whitney rank sum test. Results were defined as statistically significant, if the two-tailed $p < 0.05$. The statistical analyses and graphical work were performed using SigmaPlot (version 13.0, Systat Software). The data is given as mean \pm SD.

Results

Animals

The BW of the BTX-injected mice was significantly lower than the BW of the animals in the respective Ctrl groups (Table 1). The rectus femoris muscle mass was significantly lower in the BTX-injected animals compared to the respective

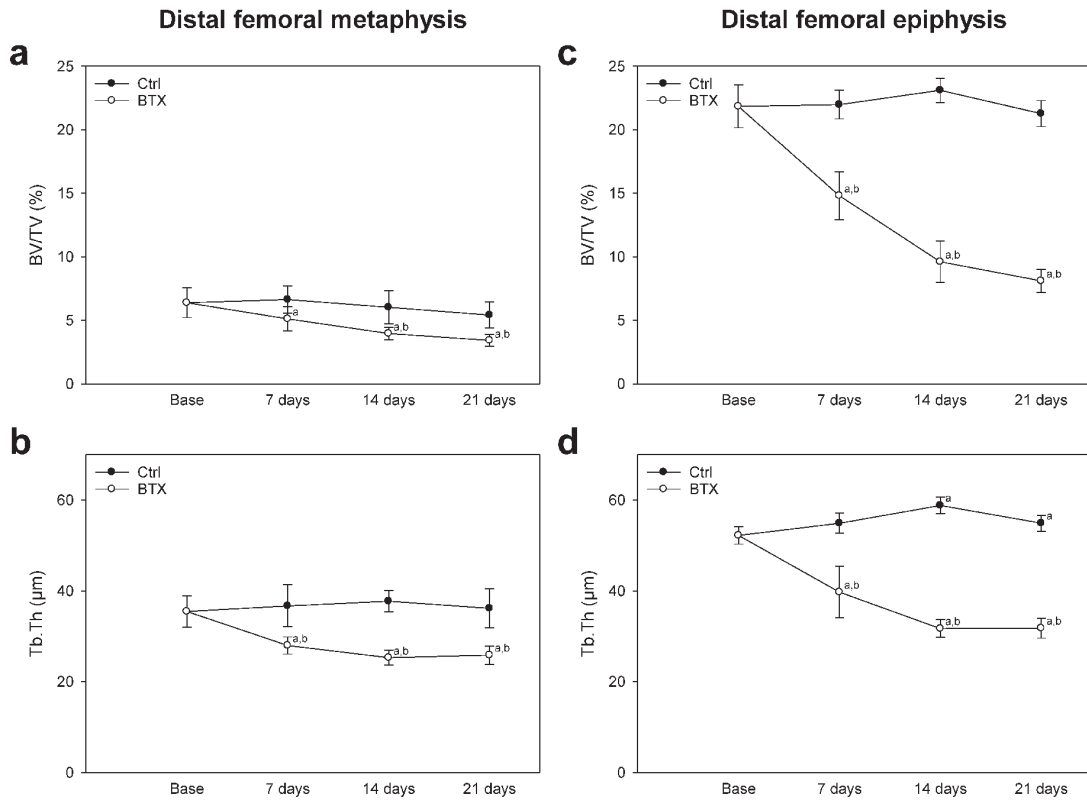


Figure 3. a: BV/TV of the distal femoral metaphysis. b: Tb.Th of the distal femoral metaphysis. c: BV/TV of the distal femoral epiphysis. d: Tb.Th of the distal femoral epiphysis. ^a denotes a significant difference from the Base group and ^b denotes a significant difference from the respective Ctrl group. n=5. Mean±SD.

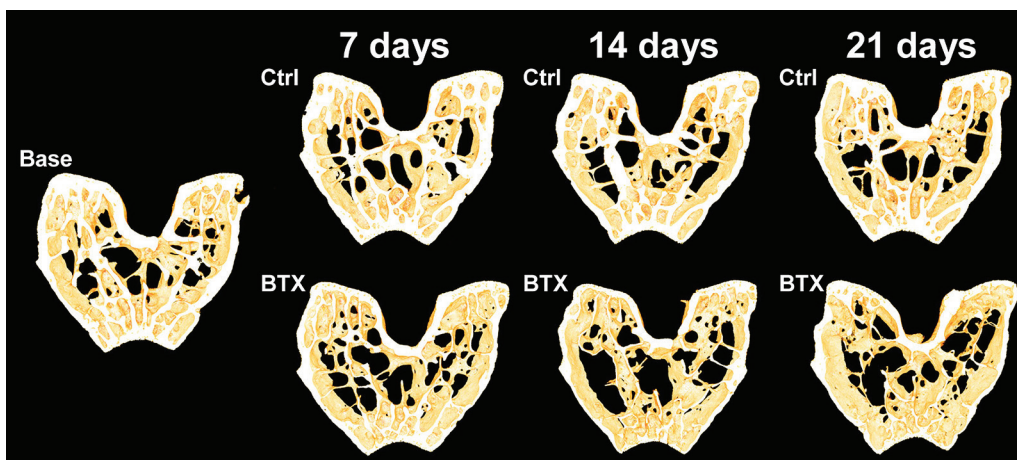


Figure 4. Representative 3D illustrations of the distal femoral epiphyses acquired from the μCT scans.

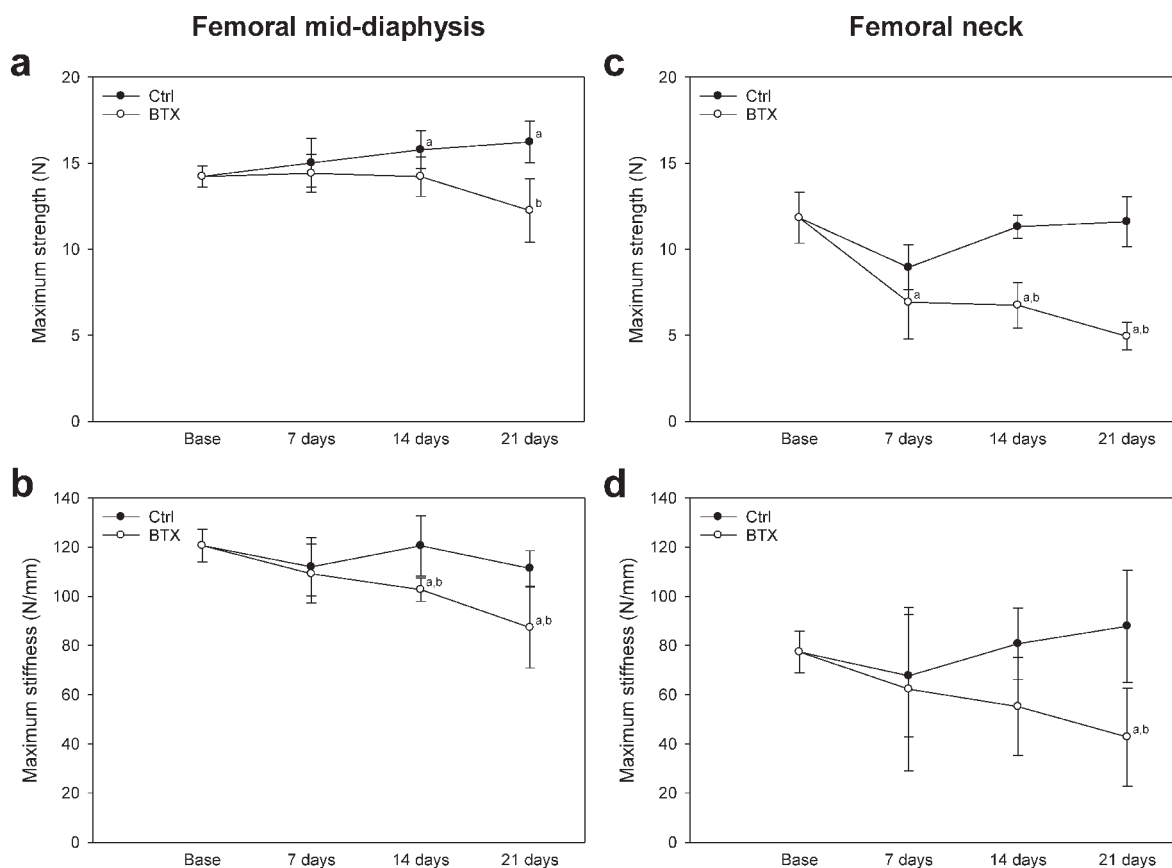


Figure 5. a: Maximum strength of the femoral mid-diaphysis. b: Maximum stiffness of the femoral mid-diaphysis. c: Maximum strength of the femoral neck. d: Maximum stiffness of the femoral neck. ^a denotes a significant difference from the Base group and ^b denotes a significant difference from the respective Ctrl group. n=5. Mean±SD.

Table 5.

	Maximum strength (N)	Maximum stiffness (N/mm)		Maximum strength (N)	Maximum stiffness (N/mm)
Femoral mid-diaphysis			Femoral neck		
Day 0			Day 0		
Base	14.2 ± 0.6	121 ± 7	Base	11.8 ± 1.5	77 ± 8
Day 7			Day 7		
Ctrl	15.0 ± 1.4	112 ± 12	Ctrl	8.9 ± 1.3	68 ± 25
BTX	14.4 ± 1.1	109 ± 12	BTX	6.9 ± 2.1 ^a	62 ± 33
Day 14			Day 14		
Ctrl	15.8 ± 1.1 ^a	121 ± 12	Ctrl	11.3 ± 0.7	81 ± 15
BTX	14.2 ± 1.1	103 ± 5 ^{a,b}	BTX	6.7 ± 1.3 ^{a,b}	55 ± 20
Day 21			Day 21		
Ctrl	16.2 ± 1.2 ^a	111 ± 7	Ctrl	11.6 ± 1.5	88 ± 23
BTX	12.3 ± 1.9 ^b	87 ± 16 ^{a,b}	BTX	4.9 ± 0.8 ^{a,b}	43 ± 20 ^{a,b}

Mechanical testing of the femoral mid-diaphysis and femoral neck. ^a denotes a significant difference from Base and ^b denotes a significant difference from the respective Ctrl group. n=5. Mean±SD.

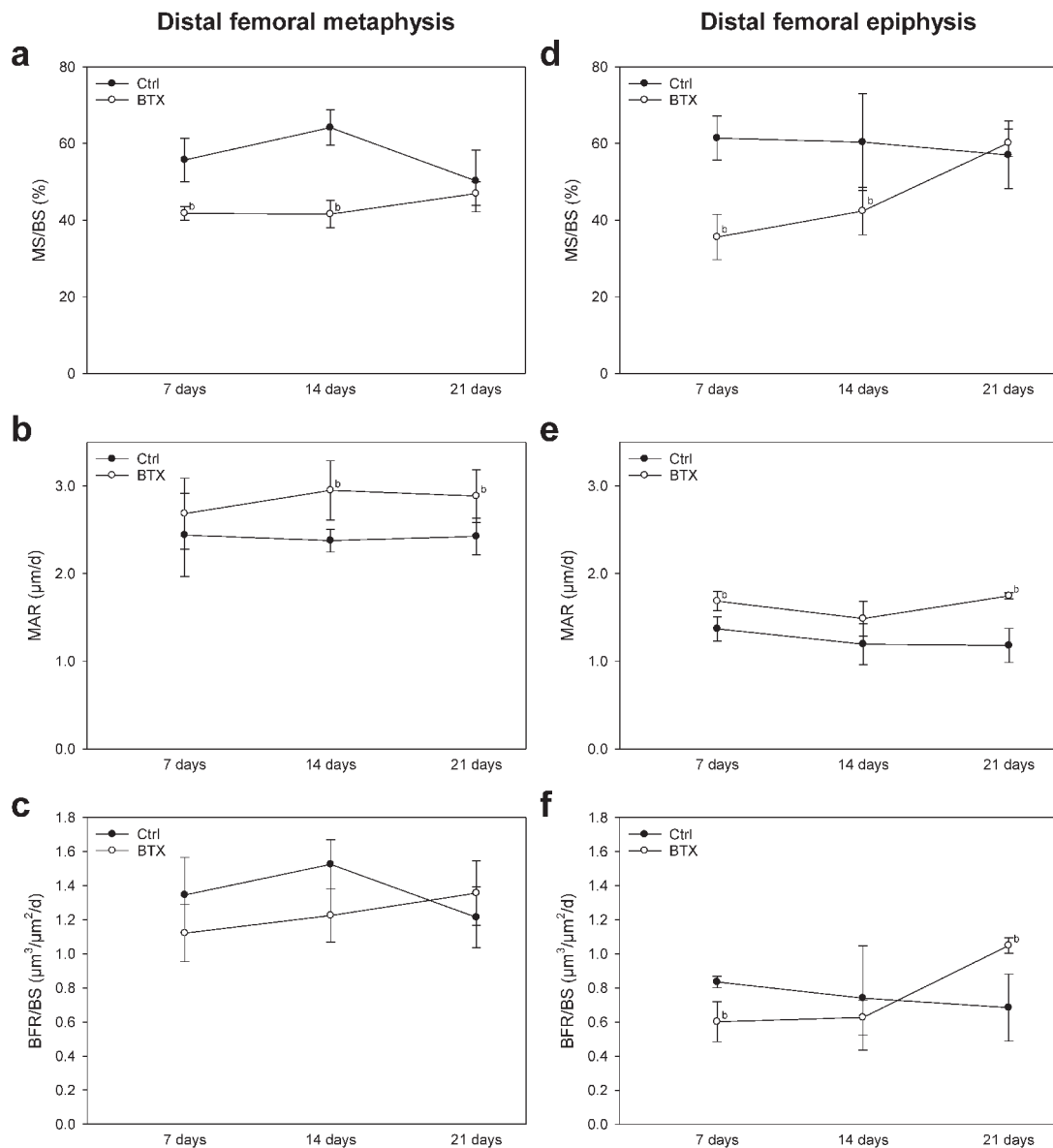


Figure 6. a: MS/BS of the distal femoral metaphysis. b: MAR at the distal femoral metaphysis. c: BFR/BS at the distal femoral metaphysis. d: MS/BS at the distal femoral epiphysis. e: MAR at the distal femoral epiphysis. f: BFR/BS at the distal femoral epiphysis. ^b denotes a significant difference from the respective Ctrl group. n=5. Mean±SD.

Ctrl groups (Table 1). The femur of the BTX-injected animals was significantly shorter after one week of disuse compared to the Ctrl group, but not significantly shorter than the Base group. The femur length was not affected after 14 and 21 days of disuse compared to both the Base and the respective Ctrl groups (Table 1).

Dual energy x-ray absorptiometry (DEXA)

The BTX-injected mice had significantly lower femoral BMC and aBMD compared to the respective Ctrl groups (Table 2).

Micro computed tomography (μCT)

The femoral mid-diaphysis bone area was significantly smaller after 14 and 21 days of disuse compared to the respective Ctrl groups and this was due to an expansion of the marrow area (Figure 2). See Table 3 for absolute values and values for tissue area, pMOI, and ρ .

The BV/TV at the distal femoral metaphysis was significantly lower after 14 and 21 days of immobilization compared to the respective Ctrl groups (Figure 3a). Moreover, the trabeculae at the distal femoral metaphysis were significantly

Table 6.

	MS/BS (%)	MAR ($\mu\text{m}/\text{d}$)	BFR/BS ($\mu\text{m}^3/\mu\text{m}^2/\text{d}$)		MS/BS (%)	MAR ($\mu\text{m}/\text{d}$)	BFR/BS ($\mu\text{m}^3/\mu\text{m}^2/\text{d}$)
Distal femoral metaphysis				Distal femoral epiphysis			
Day 7				Day 7			
Ctrl	0.56 \pm 0.06	2.44 \pm 0.47	1.35 \pm 0.22	Ctrl	0.61 \pm 0.06	1.37 \pm 0.14	0.84 \pm 0.03
BTX	0.42 \pm 0.02 b	2.68 \pm 0.41	1.12 \pm 0.17	BTX	0.36 \pm 0.06 b	1.69 \pm 0.11 b	0.60 \pm 0.12 b
Day 14				Day 14			
Ctrl	0.64 \pm 0.05	2.38 \pm 0.13	1.52 \pm 0.14	Ctrl	0.60 \pm 0.13	1.19 \pm 0.24	0.74 \pm 0.31
BTX	0.42 \pm 0.04 b	2.95 \pm 0.34 b	1.22 \pm 0.16	BTX	0.42 \pm 0.06 b	1.49 \pm 0.20	0.63 \pm 0.10
Day 21				Day 21			
Ctrl	0.50 \pm 0.08	2.42 \pm 0.21	1.21 \pm 0.18	Ctrl	0.57 \pm 0.09	1.18 \pm 0.20	0.68 \pm 0.20
BTX	0.47 \pm 0.03	2.88 \pm 0.30 b	1.36 \pm 0.19	BTX	0.60 \pm 0.04	1.75 \pm 0.03 b	1.05 \pm 0.05 b

Dynamic bone histomorphometry obtained at the distal femoral metaphysis and distal femoral epiphysis. ^b denotes a significant difference from the respective Ctrl group. n=5. Mean \pm SD.

Table 7.

	$\Delta\text{Ct Bglap}$	$\Delta\text{Ct Col1a1}$	$\Delta\text{Ct Runx2}$	$\Delta\text{Ct Sost}$	$\Delta\text{Ct Ctsk}$	$\Delta\text{Ct Acp5}$	$\Delta\text{Ct Rankl}$	$\Delta\text{Ct Opg}$
Day 0								
Base	-0.18 \pm 0.34	-1.73 \pm 0.40	5.61 \pm 0.18	5.71 \pm 0.38	3.58 \pm 0.38	3.23 \pm 0.35	8.69 \pm 0.20	8.76 \pm 0.36
Day 7								
Ctrl	-0.94 \pm 0.82	-2.32 \pm 0.84	5.62 \pm 0.21	5.64 \pm 0.51	3.99 \pm 0.58	3.48 \pm 0.52	8.62 \pm 0.65	8.93 \pm 0.74
BTX	1.33 \pm 0.44 ^{a,b}	-0.66 \pm 0.32 ^{a,b}	5.67 \pm 0.16	5.73 \pm 0.30	1.78 \pm 0.22 ^{a,b}	1.59 \pm 0.08 ^{a,b}	8.43 \pm 0.47	8.85 \pm 0.19
Day 14								
Ctrl	-1.32 \pm 0.50 ^a	-2.60 \pm 0.49 ^a	5.68 \pm 0.23	5.19 \pm 0.42	4.55 \pm 0.55 ^a	3.77 \pm 0.29 ^a	8.96 \pm 0.57	8.35 \pm 0.37
BTX	-0.10 \pm 0.58 ^b	-2.06 \pm 0.38	5.58 \pm 0.16	5.91 \pm 0.48 ^b	2.06 \pm 0.45 ^{a,b}	1.75 \pm 0.42 ^{a,b}	8.57 \pm 0.46	8.80 \pm 0.35
Day 21								
Ctrl	-0.27 \pm 0.54	-1.96 \pm 0.52	5.61 \pm 0.10	5.87 \pm 0.60	3.85 \pm 0.40	3.45 \pm 0.33	9.17 \pm 0.23	8.68 \pm 0.46
BTX	-0.98 \pm 0.21 ^{a,b}	-2.58 \pm 0.31 ^a	5.69 \pm 0.12	6.23 \pm 0.49	3.21 \pm 0.38 ^b	2.92 \pm 0.33 ^b	8.97 \pm 0.40	9.08 \pm 0.71

ΔCt values from RT-pPCR calculations obtained from the distal half of the tibia. The reference genes are B2m and Gapdh. ^a denotes a significant difference from Base and ^b denotes a significant difference from the respective Ctrl group. n=5. Mean \pm SD.

thinner after 7, 14, and 21 days of disuse compared to the respective Ctrl groups (Figure 3b). The ρ at the distal femoral metaphysis was significantly lower after 14 and 21 days of disuse compared to the respective Ctrl groups. See Table 4 for absolute values and values for Tb.N, Tb.Sp, CD, and SMI.

Both the BV/TV and Tb.Th at the distal femoral epiphysis were significantly lower after 7, 14, and 21 days of disuse than the respective Ctrl groups (Figures 3c, 3d, and 4). The ρ at the distal femoral epiphysis was significantly lower after 14 and 21 days of disuse compared to the respective Ctrl groups. Throughout the immobilization period the trabeculae at the distal femoral epiphysis became more rod-like com-

pared to the non-immobilized trabeculae, as indicated by a higher SMI. See Table 4 for absolute values and values for Tb.N, Tb.Sp, and CD.

Mechanical testing

The maximum strength of the femoral mid-diaphysis was significantly lower after 21 days of immobilization compared to the Ctrl group (Figure 5a). The maximum stiffness of the femoral mid-diaphysis was significantly lower after 14 and 21 days of immobilization compared to the respective Ctrl groups (Figure 5b).

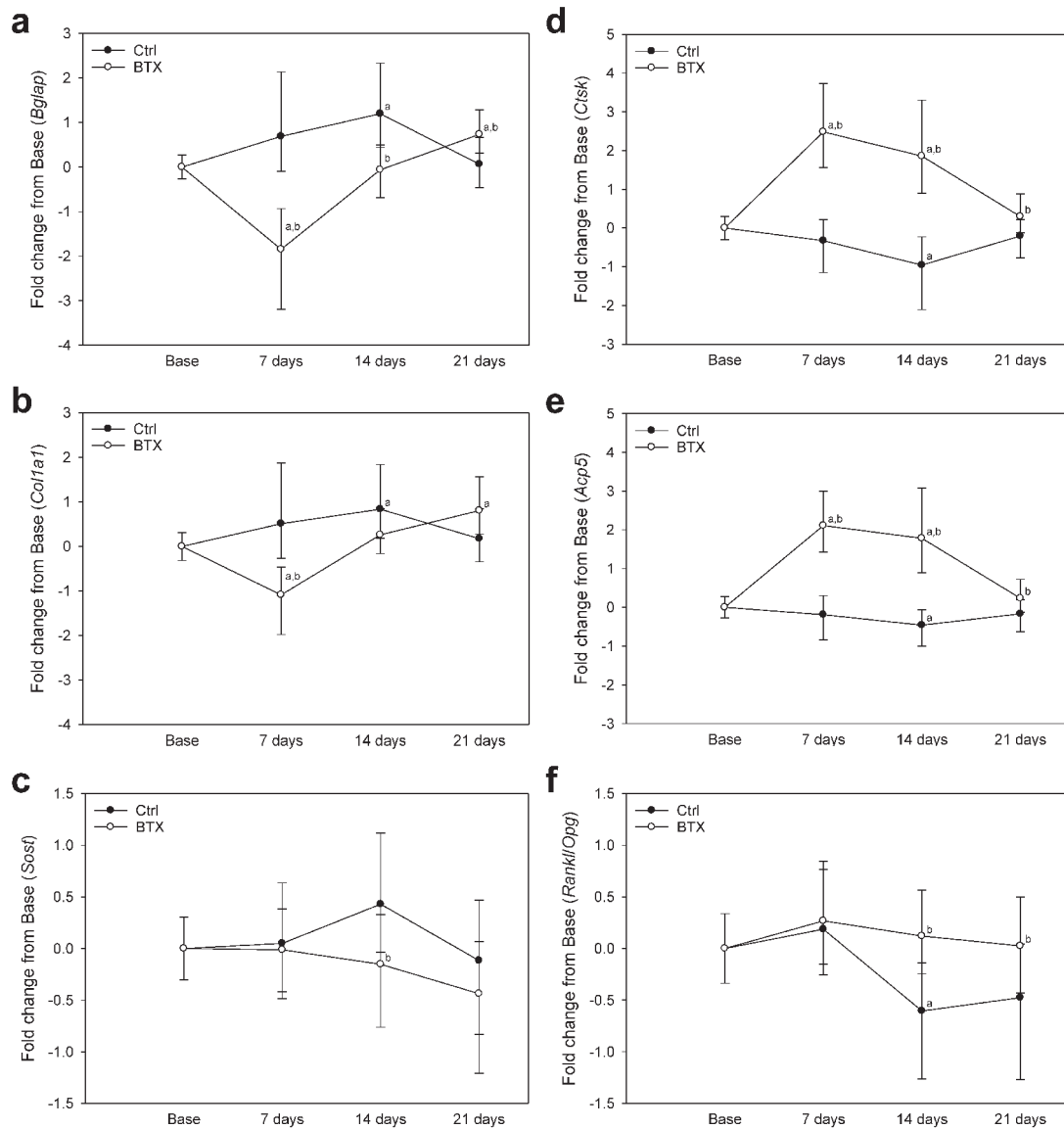


Figure 7. a: Expression of *Bglap* (osteocalcin) in the distal half of tibia. b: Expression of *Col1a1* (collagen, type 1, alpha 1) in the distal half of tibia. c: Expression of *Sost* (sclerostin) in the distal half of tibia. d: Expression of *Ctsk* (cathepsin K) in the distal half of tibia. e: Expression of *Acp5* (acid phosphatase 5, tartrate resistant) in the distal half of tibia. f: The ratio between the expression of *Rankl* (receptor activator of nuclear kappa-B ligand) and *Opg* (osteoprotegerin) i.e. the *Rankl/Opg*-ratio in the distal half of tibia. ^a denotes a significant difference from the Base group and ^b denotes a significant difference from the respective Ctrl group. n=5. Mean±SD.

The maximum strength of the femoral neck was significantly lower after 14 and 21 days of immobilization compared to the respective Ctrl groups (Figure 5c). The maximum stiffness of the femoral neck was significantly lower after 21 days of immobilization compared to the Ctrl group (Figure 5d). See Table 5 for absolute values for mechanical testing.

Dynamic bone histomorphometry

The MS/BS at the distal femoral metaphysis was significantly lower after 7 and 14 days of immobilization compared to the respective Ctrl groups (Figure 6a). The MAR was significantly higher after 14 and 21 days of immobilization compared to the respective Ctrl groups (Figure 6b). In contrast, the BFR/BS was not influenced by immobilization (Figure 6c).

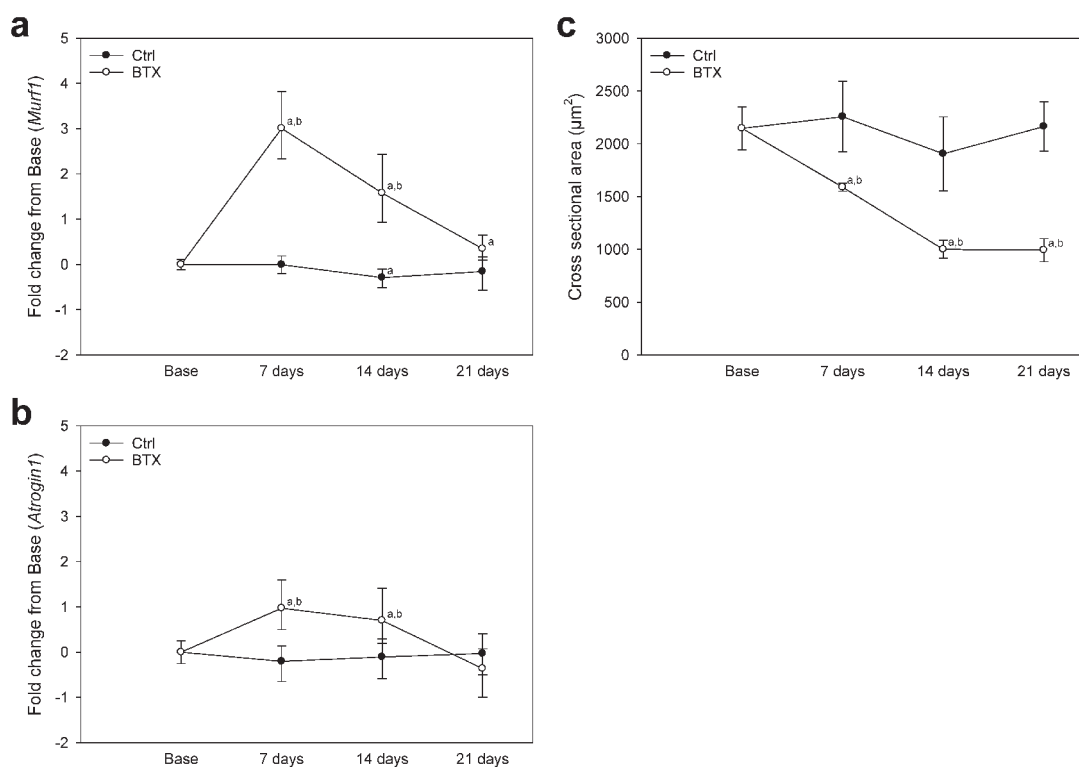


Figure 8. a: Expression of *Murf1* (tripartite motif-containing 63) in the rectus femoris muscle. b: Expression of *Atrogin1* (F-box protein 32) in the rectus femoris muscle. c: CSA of the rectus femoris muscle cells. ^a denotes a significant difference from the Base group and ^b denotes a significant difference from the respective Ctrl group. n=5. Mean±SD.

The MS/BS at the distal femoral epiphysis was significantly lower after 7 and 14 days of disuse compared to the respective Ctrl groups (Figure 6d). The MAR was significantly higher after 7 and 21 days of immobilization compared to the respective Ctrl groups (Figure 6e). The BFR/BS was significantly lower after 7 days and significantly higher after 21 days of immobilization compared to the respective Ctrl groups (Figure 6f). See Table 6 for absolute values for dynamic bone histomorphometry.

RT-qPCR

Bglap was significantly lower after 7 and 14 days, whereas it was significantly higher after 21 days of immobilization compared to the respective Ctrl groups (Figure 7a). *Col1a1* was significantly lower after 7 days of disuse compared to the respective Ctrl group (Figure 7b). *Sost* was significantly lower after 14 days of immobilization compared to the Ctrl group (Figure 7c). Both *Ctsk* and *Acp5* were significantly higher after 7, 14, and 21 days of immobilization compared to the respective Ctrl groups (Figures 7d and 7e). The *Rankl/Opg*-ratio was significantly higher after 14 and 21 days of immobilization compared to the respective Ctrl groups (Figure 7f). See Table 7 for Δ Ct values.

Table 8.

	Δ Ct <i>Murf1</i>	Δ Ct <i>Atrogin1</i>	CSA (μm^2)
Day 0			
Base	-5.29±0.16	-5.73 ±0.32	2147 ±204
Day 7			
Ctrl	-5.28±0.20	-5.46 ±0.32	2257 ±333
BTX	-7.29±0.22 ^{a,b}	-6.71 ±0.24 ^{a,b}	1590 ±38 ^{a,b}
Day 14			
Ctrl	-4.92±0.16 ^a	-5.58 ±0.40	1906 ±350
BTX	-6.66 ±0.38 ^{a,b}	-6.49 ±0.39 ^{a,b}	1001 ±85 ^{a,b}
Day 21			
Ctrl	-5.08 ±0.41	-5.68 ±0.43	2164 ±235
BTX	-5.72 ±0.25 ^a	-5.28 ±0.45	994 ±110 ^{a,b}

Δ Ct values from RT-pPCR calculations and muscle cell cross sectional area (CSA) obtained from the rectus femoris muscle. The reference gene is *Tbp*. ^a denotes a significant difference from Base and ^b denotes a significant difference from the respective Ctrl group. n=5. Mean±SD.

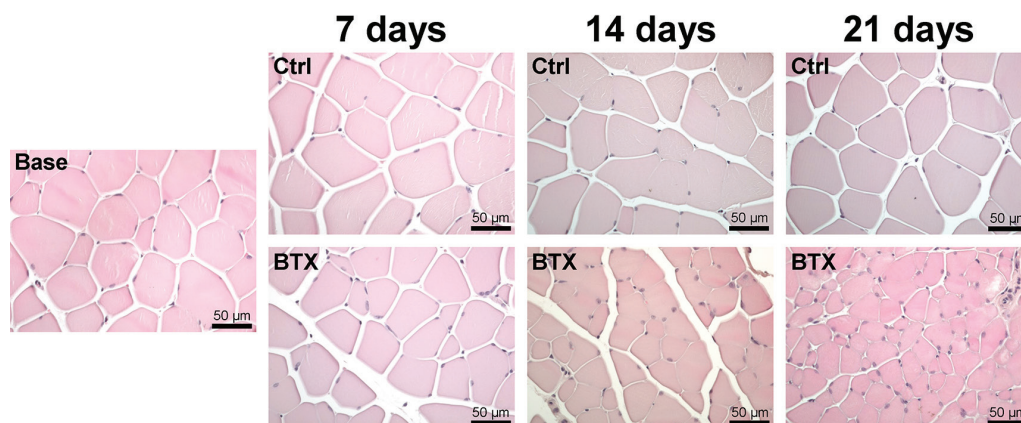


Figure 9. Representative pictures of the rectus femoris muscle cross sections acquired in the light microscope at a magnification of $\times 1170$.

Murf1 and *Atrogin1* were significantly higher after 7 and 14 days of disuse compared to the respective Ctrl groups (Figures 8a and 8b). See Table 8 for ΔCt values.

CSA of rectus femoris muscle cells

The CSA of the rectus femoris muscle cells was significantly lower 7, 14, and 21 days after the BTX-injection compared to the respective Ctrl groups (Figures 8c and 9). See Table 8 for absolute values.

Discussion

In general, the present study showed that changes in expression of genes related to bone formation and resorption, and muscle atrophy were seen during the first two weeks of immobilization. This was accompanied by changes in bone architecture, bone strength and muscle size, which, however, was most pronounced after three weeks of immobilization.

The deterioration in microstructure at both the distal femoral metaphysis and epiphysis was most evident after 21 days of immobilization, where the BTX-induced loss of BV/TV and Tb.Th was most pronounced at the distal femoral epiphysis. Likewise, in the BTX-injected mice, the reduction in bone area at the femoral mid-diaphysis was most notable after 21 days of disuse. The immobilization-induced bone loss was followed by a reduction in bone strength at both the femoral mid-diaphysis and neck. Taken together these findings suggest that bone microstructure and strength should be investigated 21 days after the BTX-injection.

Expression of *Bglap* was lower in the BTX-injected animals than in the control animals after 7 days of disuse. However, after 21 days of immobilization the expression of *Bglap* increased to a level that was significantly higher than for both baseline and control animals. This indicates a BTX-induced suppressed production of osteocalcin and bone formation

during the initial phases of the immobilization and a recovered bone formation in the later stages of the immobilization. A similar, but not as pronounced pattern was observed for *Col1a1*. In accordance, Marchand-Libouban et al. found that the expression of *Alp* (alkaline phosphatase) in BTX immobilized femora was significantly lower after 7 and 14 days compared to the contralateral non-injected femora²⁷. The expression of *Bglap* and *Col1a1* correlates with dynamic bone histomorphometry, where MS/BS was significantly lower after 7 and 14 days of disuse and not different from controls after 21 days. In agreement, BFR/BS at the distal femoral epiphysis was significantly lower after 7 days of immobilization, but significantly higher after 21 days compared to non-immobilized mice.

Ctsk and *Acp5* were notably and significantly more highly expressed in the immobilized mice after both 7 and 14 days, but approached the expression of control mice after 21 days of disuse. The elevated expression of *Ctsk* and *Acp5* indicates a higher production of cathepsin K and TRAP and hence bone resorption during the first two weeks of the immobilization. This is consistent with the notion that the rate of bone loss seems to reduce between 2 and 3 weeks of immobilization. Counterintuitively, the *Rankl/Opg*-ratio, which favors osteoclast differentiation and activity²¹ was significantly higher after 14 and 21 days of disuse compared to controls, although both bone loss and expression of *Ctsk* and *Acp5* leveled out after 21 days. We were not able to detect any significant differences in the expression of *Sost*, *Runx2*, *Rankl*, and *Opg* between the BTX-injected and control animals. This might be due to a missed detection window if changes in the expression of these genes happened between day 0 to 7 of immobilization, insensitivity of the RT-qPCR method and assay, or the tissue preparation as earlier suggested²⁸. In fact, after the injection of BTX in rats, Macias et al. found that the expression of *Sost* during the early phase of bone loss was upregulated in diaphyseal bone, but downregulated in metaphyseal bone

suggesting complicated and paradoxical bone site specific gene expression patterns²⁹. This might explain why we were not able to detect substantial changes in the expression of *Sost*, as we used the distal half of tibia for RT-qPCR, which includes both diaphyseal and metaphyseal bone.

In the present study we have shown that in mice, changes in bone cell related gene expression take place during the first two weeks of immobilization, whereas the deterioration of microarchitecture and bone strength is most evident after three weeks of immobilization. Thus, analyzing gene expression after three weeks of disuse is fruitless as expression levels are similar in the BTX-injected animals and the control animals. In a worst case scenario, genes related to osteoclasts are similar in BTX-injected and control animals, whereas osteoblast related genes might be higher expressed in BTX-injected mice after 3 weeks of disuse. This suggests that it is not optimal to investigate both gene expression and bone structure at the same time-point. Therefore, when designing an interventional unloading study, a subpopulation for RT-qPCR should be included and investigated to an earlier time-point.

In the rectus femoris muscle, the expression of *Murf1* and *Atrogin1* was higher after 7 and 14 days of disuse, but was not different from control animals after 21 days of disuse. In contrast, the muscle weight and muscle cell CSA were most affected 21 days after the BTX-injections. This is consistent with the relationship between bone cell related gene expression and bone loss during immobilization. Therefore, the optimal time-point for analysis of these parameters depends on whether molecular or structural investigations are of interest in BTX-induced muscle atrophy.

In conclusion, gene expression and dynamic bone histomorphometry alterations precede deterioration in parameters obtained by DEXA, μ CT, and mechanical testing. Therefore, the best time-point for investigating gene expression patterns in BTX-induced bone loss is during the first two weeks of immobilization, whereas DEXA, μ CT, and mechanical testing should be performed after three weeks of immobilization. This is also the case when investigating atrophy related gene expression in BTX-induced muscle atrophy, where gene expression is affected in the first two weeks after the BTX-injection, whereas muscle weight and muscle cell CSA deterioration is most evident after three weeks of immobilization.

Acknowledgements

The authors are grateful for the hard work and excellent technical assistance of Jytte Utoft. We thank Visiopharm for the contribution to the newCAST stereology software system and the Velux Foundation for the donation of the μ CT scanner.

References

- Allison N, Brooks B. Bone atrophy: an experimental and clinical study of the changes in bone which result from non-use. *Surg Gynecol Obstet* 1921;33:250-60.
- Morey ER, Sabelman EE, Turner RT, Baylink DJ. A new rat model simulating some aspects of space flight. *Physiologist* 1979;22: 23-4.
- Lindgren U. The effect of thyroparathyroidectomy: development of disuse osteoporosis in adult rats. *Clin Orthop Relat Res* 1976;333:251-6.
- Chappard D, Chennebault A, Moreau M, Legrand E, Audran M, Basle MF. Texture analysis of X-ray radiographs is a more reliable descriptor of bone loss than mineral content in a rat model of localized disuse induced by the Clostridium botulinum toxin. *Bone* 2001;28:72-9.
- Vegger JB, Nielsen ES, Brüel A, Thomsen JS. Additive effect of PTH (1-34) and zoledronate in the prevention of disuse osteopenia in rats. *Bone* 2014;66:287-95.
- Lodberg A, Vegger JB, Jensen MV, Larsen CM, Thomsen JS, Brüel A. Immobilization induced bone loss is strain specific in mice. *Bone Reports* 2015;2:59-67.
- Brüel A, Vegger JB, Raffalt AC, Andersen JET, Thomsen JS. PTH (1-34), but not strontium ranelate counteract loss of trabecular thickness and bone strength in disuse osteopenic rats. *Bone* 2013;53:51-8.
- Thomsen JS, Christensen LL, Vegger JB, Nyengaard JR, Brüel A. Loss of bone strength is dependent on skeletal site in disuse osteoporosis in rats. *Calcif Tissue Int* 2012;90:294-306.
- Vegger JB, Brüel A, Thomsen JS. Vertical trabeculae are thinned more than horizontal trabeculae in skeletal-unloaded rats. *Calcif Tissue Int* 2015;97:516-26.
- Warner SE, Sanford DA, Becker BA, Bain SD, Srinivasan S, Gross TS. Botox induced muscle paralysis rapidly degrades bone. *Bone* 2006;38:257-64.
- Grubbe MC, Thomsen JS, Nyengaard JR, Duruox M, Brüel A. Growth hormone mitigates loss of periosteal bone formation and muscle mass in disuse osteopenic rats. *J Musculoskelet Neuronal Interact* 2014;14:473-83.
- Manske SL, Boyd SK, Zernicke RF. Muscle and bone follow similar temporal patterns of recovery from muscle-induced disuse due to botulinum toxin injection. *Bone* 2010;46:24-31.
- Grimston SK, Silva MJ, Civitelli R. Bone loss after temporarily induced muscle paralysis by botox is not fully recovered after 12 weeks. *Ann N Y Acad Sci* 2007; 1116:444-60.
- Kruse K, Kracht U. Evaluation of serum osteocalcin as an index of altered bone metabolism. *Eur J Pediatr* 1986;145:27-33.
- Xiao G, Jiang D, Thomas P, Benson MD, Guan K, Karsenty G, et al. MAPK pathways activate and phosphorylate the osteoblast-specific transcription factor, Cbfa1. *J Biol Chem* 2000;275:4453-9.
- Li X, Zhang Y, Kang H, Liu W, Liu P, Zhang J, et al. Sclerostin binds to LRP5/6 and antagonizes canonical Wnt signaling. *J Biol Chem* 2005;280:19883-7.
- Winkler DG, Sutherland MK, Geoghegan JC, Yu C, Hayes T, Skonier JE, et al. Osteocyte control of bone formation via sclerostin, a novel BMP antagonist. *EMBO J* 2003;22:6267-76.
- Lin C, Jiang X, Dai Z, Guo X, Weng T, Wang J, et al. Sclerostin mediates bone response to mechanical unloading

- through antagonizing Wnt/ β -Catenin signaling. *J Bone Miner Res* 2009;24:1651-61.
19. Drake FH, Dodds RA, James IE, Connor JR, Debouck C, Richardson S, et al. Cathepsin K, but not cathepsins B, L, or S, is abundantly expressed in human osteoclasts. *J Biol Chem* 1996;271:12511-6.
 20. Minkin C. Bone acid phosphatase: tartrate-resistant acid phosphatase as a marker of osteoclast function. *Calcif Tissue Int* 1982;34:285-90.
 21. Lacey DL, Timms E, Tan HL, Kelley MJ, Dunstan CR, Burgess T, et al. Osteoprotegerin ligand is a cytokine that regulates osteoclast differentiation and activation. *Cell* 1998;93:165-76.
 22. Bodine SC, Baehr LM. Skeletal muscle atrophy and the E3 ubiquitin ligases *MuRF1* and *MAFbx/atrogen-1*. *AJP Endocrinol Metab* 2014;307:469-84.
 23. Bouxsein ML, Boyd SK, Christiansen BA, Guldberg RE, Jepsen KJ, Müller R. Guidelines for assessment of bone microstructure in rodents using micro-computed tomography. *J Bone Miner Res* 2010;25:1468-86.
 24. Thomsen JS, Laib A, Koller B, Prohaska S, Mosekilde L, Gowin W. Stereological measures of trabecular bone structure: comparison of 3D micro computed tomography with 2D histological sections in human proximal tibial bone biopsies. *J Microsc* 2005;218:171-9.
 25. Schmittgen TD, Livak KJ. Analyzing real-time PCR data by the comparative CT method. *Nat Protoc* 2008;3:1101-8.
 26. Nakao R, Yamamoto S, Yasumoto Y, Kadota K, Oishi K. Impact of denervation-induced muscle atrophy on housekeeping gene expression in mice. *Muscle Nerve* 2015;51:276-81.
 27. Marchand-Libouban H, Le Drévo MA, Chappard D. Disuse induced by botulinum toxin affects the bone marrow expression profile of bone genes leading to a rapid bone loss. *J Musculoskelet Neuronal Interact* 2013;13:27-36.
 28. Kelly NH, Schimenti JC, Patrick Ross F, van der Meulen MCH. A method for isolating high quality RNA from mouse cortical and cancellous bone. *Bone* 2014;68:1-5.
 29. Macias BR, Aspenberg P, Agholme F. Paradoxical *Sost* gene expression response to mechanical unloading in metaphyseal bone. *Bone* 2013;53:515-9.